



# Effects of concrete strength and steel reinforcement area on the mechanical performance of functionally graded reinforced concrete beams: experimental and numerical investigation

Seleem S. E. Ahmad, Esraa Ali, Hesham Elemam, Mohamed Moawad

*Faculty of Engineering, Zagazig University, Egypt*

*seleemahmad62@yahoo.com, <http://orcid.org/0000-0001-9894-0209>*

*esraaalinassar2020@gmail.com, <http://orcid.org/0000-0002-8558-066X>*

*elemamb@missouri.edu, <http://orcid.org/0000-0002-7685-2985>*

*mamoawad@zu.edu.eg, <http://orcid.org/0000-0002-6806-900X>*

**ABSTRACT.** In this work, an experimental and numerical program was designed to evaluate the role of compressive strength,  $F_c$ , and area of reinforcing steel,  $A_s$ , on the flexural behavior of functionally graded reinforced concrete beams. Eighteen layered sections of reinforced concrete beams were tested with different compressive strengths arrangement and area of main steel. The result showed that the minimum steel reinforcement with higher compressive strength in the compression zone increases load capacity and ductility up to 31.3% and 37.1% respectively. The average steel reinforcement with higher strength in the compression zone increases load capacity and decreases ductility. The increase in load capacity was 8.3% and the decrease in deflection was 30.3%. The results also approved that; higher strength in the compression zone can be used in beams with a high tensile steel ratio for decreasing compression steel as an economic side. 3D finite element was executed using ABAQUS to simulate experimental beams. The numerical and experimental results in the present work showed a similar behavior but there are slight differences between their values.

**KEYWORDS:** Compressive strength, Area of steel, 3D finite element, Functionally graded concrete.



**Citation:** Ahmad, S. S. E., Ali, E., Moawad, M., Elemam, H., Effects of concrete strength and steel reinforcement area on the mechanical performance of functionally graded reinforced concrete beams: experimental and numerical investigation, *Frattura ed Integrità Strutturale*, 65 (2023) 270-288

**Received:** 17.04.2023

**Accepted:** 15.06.2023

**Online first:** 17.06.2023

**Published:** 01.07.2023

**Copyright:** © 2023 This is an open access article under the terms of the CC-BY 4.0, which permits unrestricted use, distribution, and reproduction in any medium, provided the original author and source are credited.

## INTRODUCTION

High strength concrete, HSC, has been easily used in building construction. However, its brittle behavior remains an obstacle to using it. HSC can be used in compression structural elements (like columns) to reduce their cross-section and reinforcement steel. HSC can be used in elements subjected to bending moment, which gives higher load capacity compared to normal concrete, in addition, to minimizing deflection and fracture in a brittle manner, so HSC



can be constructed as a part of an element for getting high load capacity with a deflection ensure serviceability limit state. That concept of construction is applied in functionally graded concrete, FGC, [1].

Experimental work was done using FGC with two types of concrete, one with Steel fiber and another with Polypropylene fiber with three different ratios of 0.5, 1, and 2%, and different configurations of concrete in the cross section. The best performance in a single type of concrete was found when using a 2% percentage of steel fiber and for FGC using steel fiber in the tension zone and Polypropylene fiber in the compression zone with 1%, which was preferred in performance and economy [2].

Another concept of FGC by using a layer of lightweight concrete around the neutral axis in-between compressive fiber reinforced concrete, FRC, or normal concrete and tensile layer FRC. The result showed that flexural strength ranges between 94-100 percent of the beam full depth with the same concrete type FRC. Using FRC in the tension and compression zone gives higher toughness than using FRC in the tension zone only.[3]

Unreinforced concrete beams' flexural strength is affected by compressive strength in tension and compression zones. Different thicknesses of layered concrete Normal strength concrete (NSC) and fiber-reinforced geopolymer (FRG) with different ratios of fiber (0, 1.5, 3%) were studied. Using FRG in the tension zone enhanced flexural strength and toughness regardless of the ratio of fiber used. Flexural strength enhancement was 87.4% when using half thickness layer of FRG compared to the whole section of NSC[4].

Flexural strength and ductility of concrete beams are controlled by reinforcing steel in compression and tension, also concrete grade. Using a higher grade of concrete gives a limited increase in the strength and ductility of concrete beams. Same as using steel in a compression zone with constant tension steel, which increases flexural ductility with little increase in strength. Using a combined increase in tension and compression steel produces a significant increase in flexural strength without decreasing ductility [5], [6].

For structural members subjected to bending moment and resisting high load capacity with a small section, HSC can be used for resisting load. However, its brittle failure or increasing main steel reinforcement leads to a reduction in element ductility. Mansor et al. studied beams' strength, ductility, and deflection with different ratios of main steel reinforcement. It was concluded that the displacement ductility index decreases as the ratio of main reinforcement increase with a sharp reduction in the high ratio. At specific load in the elastic range, the deflection of beams was affected by the steel ratio. A higher ratio of steel records low deflection as the same at max load. [7].

Another study showed different ratios of main steel reinforcement with different types of confinement in the compression zone. The result showed that confining compression zone with steel fiber and carbon fiber reinforced polymer sheet (CFRPs) gives higher load capacity than reinforced concrete without confinement, in addition to increasing the ductility of beams for all reinforcement ratios [8].

Strengthening of beams with high-strength stainless steel wire rope (HSSWR) is also affected the by steel reinforcement ratio. Ke Li et al. studied strengthened beams with HSSWR using different ratios of steel reinforcement. The result showed that the failure mode of strengthened beams was concrete crushing followed by reinforcement layer rupture when using a low steel reinforcement ratio, while using high steel reinforcement the failure was concrete crushing without reinforcement layer rupture [9].

Two methods have been studied for maintaining a minimum level of flexural ductility, moment curvature, and neutral axis to effective depth ratio. Studying compression zone in flexural members by adding compression reinforcements or confining compression zone or both enhances the moment capacity case of under reinforced sections and increases moment capacity and ductility for over reinforced sections [8]. Ductility according to moment curvature decreases with increasing main steel ratio but increases using compression reinforcements or confining compression zone at the same ratio. To maintain minimum flexural ductility, the curvature ductility factor not decrease than 3.22 or steel to balance ratio should be 0.75, or the neutral axis to fixed depth ratio equal 0.5 [10].

Flexural ductility and strength of concrete beams were studied using steel fiber and carbon fiber with different ratios of main steel reinforcing. The result showed that cracking, yielding, and ultimate load point increases with increasing steel fiber volume fraction; however, carbon fiber has little enhancement. The number of cracks decreases with a higher volume fraction, but flexural ductility decreases [11], [12]. Increasing concrete grade or increasing fiber volume fraction results in increasing flexural rigidity [11]. Post-cracking stiffness increase with the higher reinforcing ratio at the same time, the first cracking load decrease with higher numbers of bars [13].

In this research, experimental and numerical works will study by using different compressive strengths of concrete and different arrangements in layered sections by varying steel reinforcement ratios. The flexural strength ductility of the tested beams will be studied.

## EXPERIMENTAL PROGRAM

The experimental program consists of eighteen reinforced concrete beams. The beams' sections have two equal parts in compression and tension zones with different concrete grades (20, 35, 50 MPa), as shown in Fig. 1. Different ratios of steel reinforcement (minimum and average) were used in the tension zone. Details of all beams are listed in Tab. 1. All beams have compression steel of 2Φ10 mm and stirrups of 8 mm @ 200 mm. The reinforcement ratio was calculated based on the Egyptian Code ECP 203 2020 [14]. The average area of steel,  $A_s$ , was calculated as the average between the minimum area of steel (66 mm<sup>2</sup>) and the maximum area of steel (191.4 mm<sup>2</sup>) resulting average  $A_s$  of 257.4 mm<sup>2</sup> (2.276 Φ 12 close to 3 Φ 12). The beam dimensions (width x depth x length) are (150x250x1500) mm.

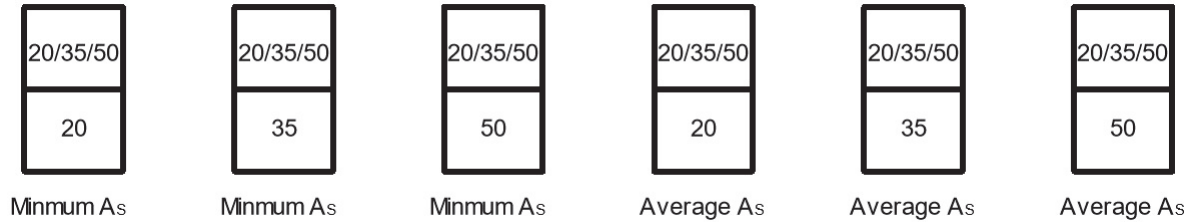


Figure 1: Beams cross section with different layer.

Beam ID	Description		Flexural rebars
	Lower part Fc, MPa	Upper part Fc, MPa	
20-20MIN	20	20	2Φ10
35-20MIN	20	35	2Φ10
50-20MIN	20	50	2Φ10
20-35MIN	35	20	2Φ10
35-35MIN	35	35	2Φ10
50-35MIN	35	50	2Φ10
20-50MIN	50	20	2Φ10
35-50MIN	50	35	2Φ10
50-50MIN	50	50	2Φ10
20-20AV	20	20	3Φ12
35-20AV	20	35	3Φ12
50-20AV	20	50	3Φ12
20-35AV	35	20	2Φ16
35-35AV	35	35	2Φ16
50-35AV	35	50	2Φ16
20-50AV	50	20	3Φ16
35-50AV	50	35	3Φ16
50-50AV	50	50	3Φ16

Table 1: Configuration of tested beams in this work.

The material used for the production of these beams were coarse aggregate with a nominal maximum aggregate size of 14 mm and grading shown in Fig. 2.a, fine aggregate with a fineness modulus of 2.4 and grading shown in Fig. 2.b, ordinary Portland cement with grade of 42.5, silica fume, superplasticizer, and steel reinforcement with diameter 8, 10, 12, and 16 mm with properties in Tab. 2 according to ISO 6935 – 2/2019 [15]. Three grades of concrete 20, 35, 50 MPa were designed using ACI 211 [16]. The material quantities per cubic meter volume are entailed in Tab. 3. The compressive strength of each mix was obtained from three cubes with dimensions 150x150x150mm according to BS EN 12390-3/2009 [17]. Tensile strength was obtained from cylinders with dimensions 150\*300mm according to BS EN 12390-6/2009[18]. All specimens were cast and tested after 28 days.

Cubes and cylinders were tested in a compression testing machine after 28 days of curing. The average results of compressive and tensile strength are shown in Tab. 4.

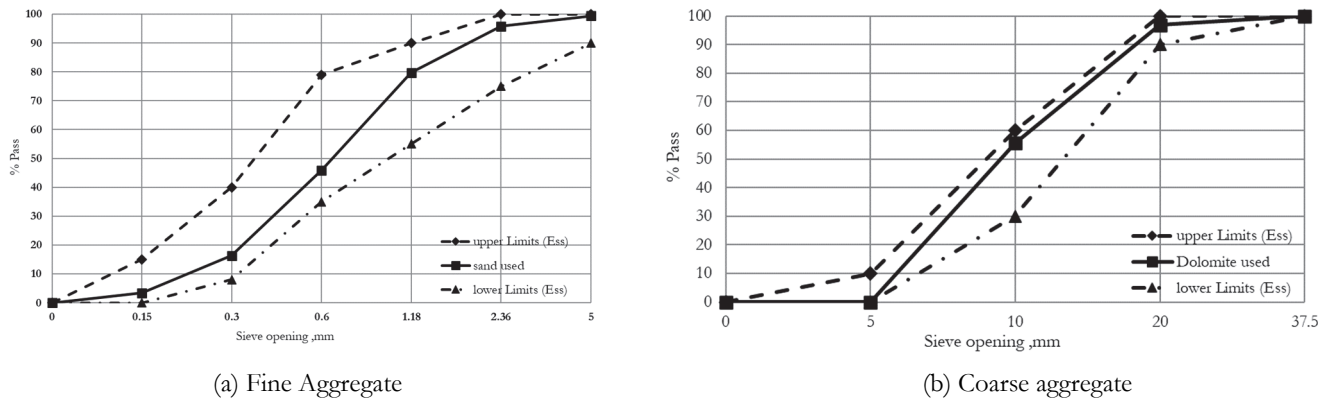


Figure 2: Grading of aggregate.

Nominal Diameter(mm)	Yield Stress (MPa)	Tensile strength (MPa)	Ultimate strain%
8	285	410	17
10	547.3	741.8	15
12	549.6	658.5	16.7
16	497.2	696	12.5

Table 2: Mechanical properties of steel.

Mix code	Cement (kg)	Dolomite (kg)	Sand (kg)	Water (Lit)	Super Plasticizer (Lit)	Silica Fume (kg)
Mix1	300	1100	788	190	--	--
Mix2	420	1100	704	180	3.36	--
Mix3	450	1100	643	165	12.5	45

Table 3: Component of cubic meter.

Mix code	Compressive strength (MPa)	Tensile strength (MPa)
Mix1	19.5	1.78
Mix2	32.5	2.64
Mix3	53.4	3.53

Table 4: Compressive and tensile strength of concrete.

## INSTRUMENTATION AND TEST SETUP

The testing of the beams was carried out on a universal testing machine capacity of 1000kN. All beams were tested under four-point bending with an effective span of 1400 mm and a shear span of 475 mm, as shown in Fig. 3. The deflection was measured at mid span using LVDT, and the load was recorded using a load cell as shown in Fig. 3 according to BS EN 12390-5/2009 [19]. Beams were monotonically tested up to failure, and cracks that appeared during the test were traced.

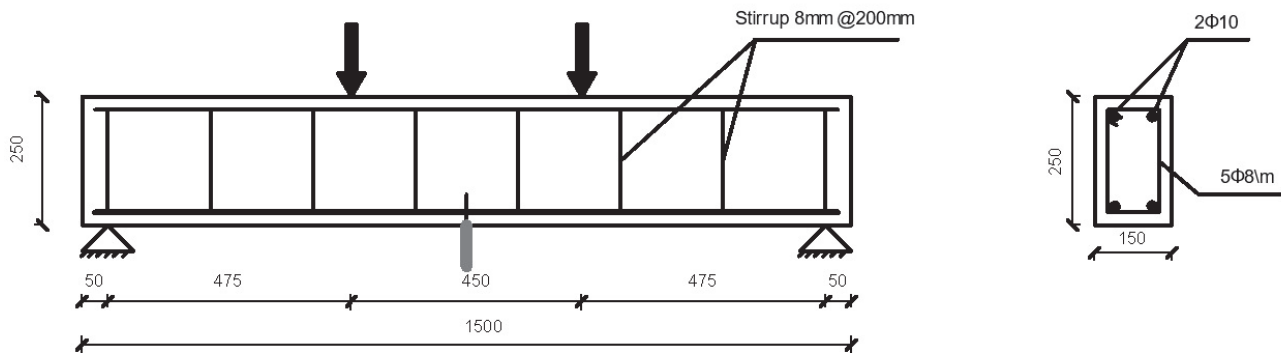


Figure 3: Beam details and loading.

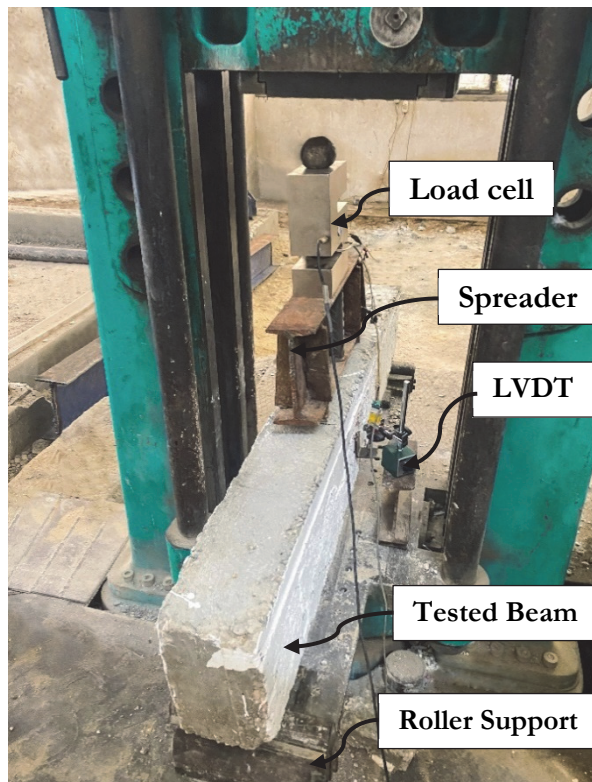


Figure 4: Test setup.

## EXPERIMENTAL TEST RESULTS AND DISCUSSION

All beams are tested up to failure, and load-deflection data, crack patterns, and modes of failures were recorded for each beam. Three different stages during beam loading were observed. The first stage was the pre-cracking of concrete, in which there was a linear relation between the load and deflection of beams. The second stage was post-cracking of concrete in which the stiffness of beams was reduced up to tension steel yielding. After that, concrete crushing or shear failure occurred according to the beam case, as will be shown in the load-deflection curves.

Fig. 5.a shows the load-deflection curve for beam ID of 20-20 Min as the control beam (concrete strength is 20 MPa for the two layers of the beam with minimum  $A_s$ ). The strength of the compression zone in the other beams was 35 or 50 MPa. It can be seen that the load carrying capacity increased from 80.3 kN to reach 81.5 kN for beam of upper layer strength equals 35MPa, with an increment of 1.5%, and from 80.3 kN to reach 105.6 kN for beam of upper layer strength equals 50 MPa, with an increment of 31.3%. A similar behavior was found for the beam's deflection, where the deflection increased from 11.1 mm to reach 12.4 mm for the beam with upper layer strength of 35 MPa with an increment of 11.7%. While the

deflection increased from 11.1 mm to reach 15 mm for the beam with upper layer strength of 50 MPa with an increment of 35.1%. It is concluded that load carrying capacity and deflection were increased with increasing strength in the compression zone.

These results can be attributed to the increasing in the strength of the upper layer with respect to the lower layer of the beam which gives a chance for main steel reinforcement of beam to make more deformations after yielding and before global failure of the beam. Similarly, the beams with average  $A_s$  show the same increase in load carrying capacity from 115 kN to 120.8 kN with strength 50 MPa with an increment of 5.6% despite strength 35 MPa having no difference in loads. The deflection of beams decreased from 9.04 mm to 7.08 mm with a strength 35 MPa with an increment of 21.6% and from 9.04 mm to 6.3 mm with a strength 50 MPa with an increment of 30.3%. It is concluded that load carrying capacity with increasing strength in the compression zone however, deflection decrease with increasing strength, as shown in Fig. 5.b.

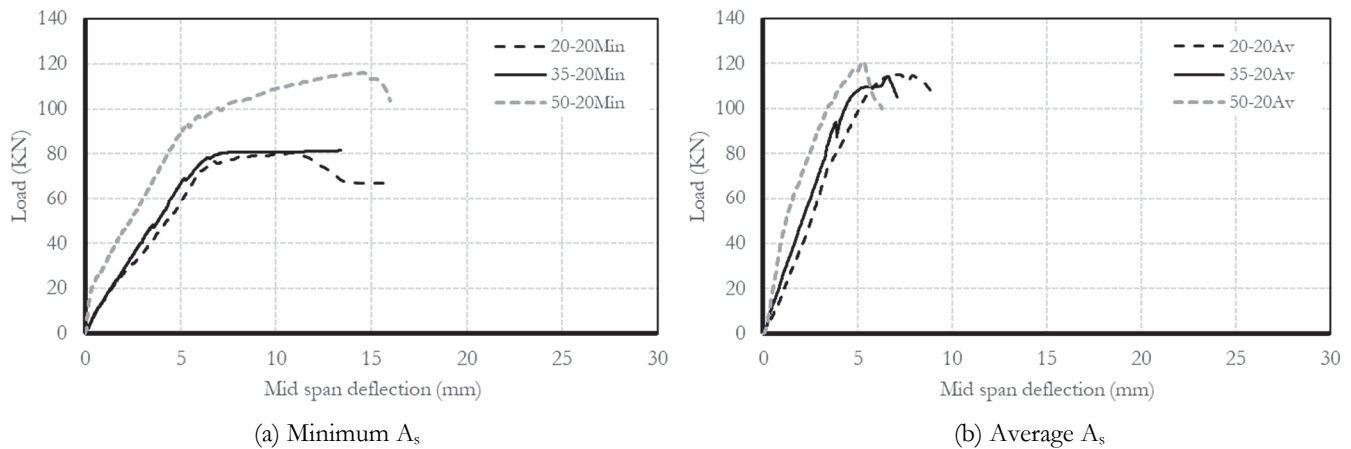


Figure 5: Load-deflection curve using concrete strength 20 MPa in tension zone and variation in Compression zone.

Steel reinforcement ratio was studied in beams that have the same layer with different reinforcement ratios. All beams with an average steel reinforcement ratio have higher load carrying capacity and lower ductility than the same minimum steel reinforcement ratio. The load capacity increased from 80.3 kN to 115.2 kN with an increment of 43.4% case, and the deflection decreased from 11.1 mm to 9 mm with an increment of 18.5% in beam 20-20 Min to Av respectively.

Similarly, for beams 35-20 Min and Av, the load capacity increased from 81.5 kN to 114.3 kN with an increment of 40.4%. The deflection decreased from 13.4 mm to 7.1 mm with an increment of 47.2%. In beams 50-20 Min and Av, the load capacity has slightly increased with an increment of 42%. The deflection decreased from 15.9 mm to 6.3 mm with an increment of 60.6%. It is concluded that increasing the tensile steel reinforcement ratio gives a higher increase in load carrying capacity at the same time, decreasing beam ductility, as shown in Fig. 6. The failure modes of these beams are shown in Fig. 7. Regardless of the maximum deflection, all beams failed due to shear. Unlike the beams with average steel, the beams with a minimum steel showed a pronounced deflection after yielding up to failure.

Fig. 8.a shows the load-deflection curve using beam 35-35Min as the control beam (Concrete strength 35 MPa with minimum  $A_s$ ). The strength of the compression zone in the other beams was 20 or 50 MPa. It was shown that the load capacity of beams slightly increased with compressive strength 50 MPa with an increment of 5.23% and decreased with strength 20MPa with an increment of 0.34%. The deflection increases from 14 mm to 16.1 mm with compressive strength 20 MPa with an increment of 14.8% and from 14 mm to 22.3 mm with compressive strength 50 MPa with an increment of 37.1%. It is concluded that higher strength in the compression zone increases the load carrying capacity and deflection.

Similarly, the beams with average  $A_s$  show a slight increase in load carrying capacity from 148.6 kN to 162.1kN with compressive strength of 50 MPa of a percentage of 8.3% and increasing of a percentage of 1.2% with compressive strength of 20 MPa. The deflection decreased by 1.4% with a strength of 20 MPa and 2.6% with a strength of 50 MPa. It is concluded that higher strength in the compression zone increases load carrying capacity and decreases deflection, as shown in Fig. 8.b.

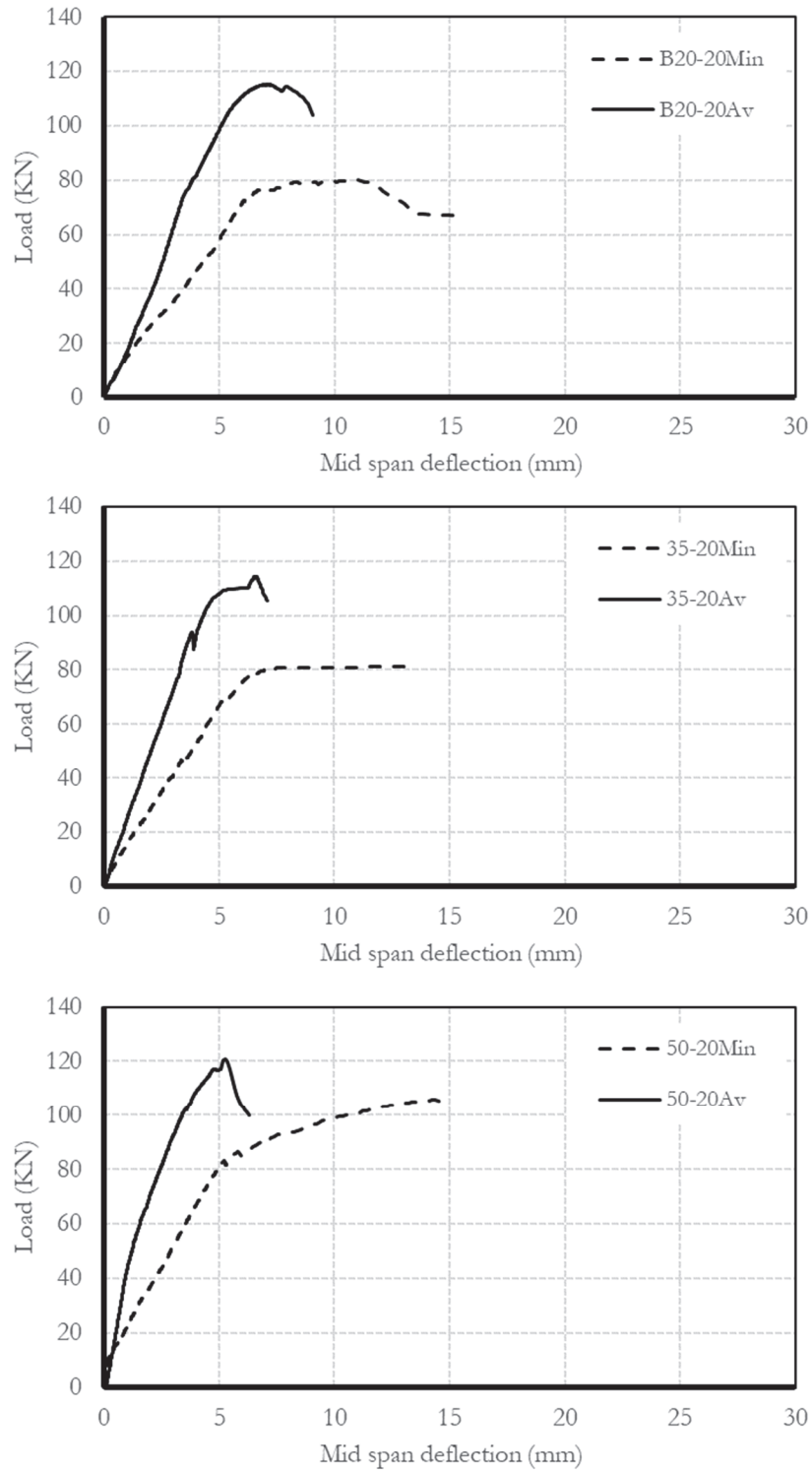


Figure 6: Load-deflection curve for beams with the same layers of beam section and different  $A_s$ .



Figure 7: Crack pattern using concrete strength 20 MPa in tension zone and variation in Compression zone.

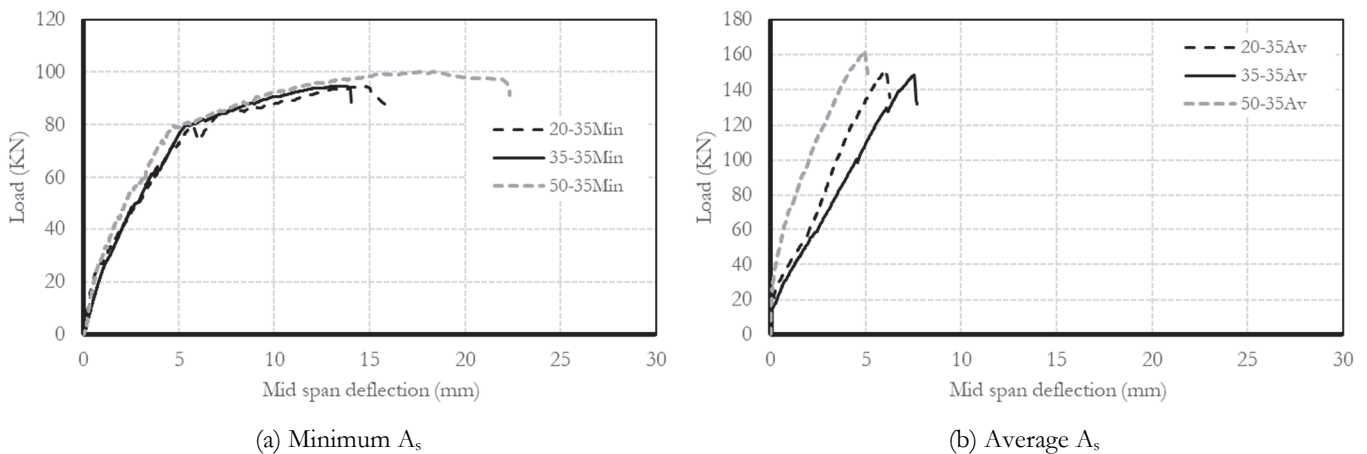


Figure 8: Load-deflection curve using concrete strength 35 MPa in tension zone and variation in Compression zone.

For the beams having the same layers and different reinforcement ratios, average steel reinforcement ratios achieved higher load carrying capacity and lower ductility than the same minimum steel reinforcement ratios. The load capacity increased from 94.3 kN to 150.3 kN with an increment of 59.3%, and deflection decreased from 16.1 mm to 9.8 mm with an increment of 61.1% in beam 20-35 Min and Av. In beam 35-35Min and Av, the load carrying capacity increased from 94.7 kN to 148.6 kN with an increment of 56.8%, and the deflection decreased from 14 mm to 7.7 mm with an increment of 45.1%. Similarly, beams 50-35 Min and Av. The load carrying capacity increased from 100 kN to 162.1 kN with an increment of 71.8%, and the deflection decreased from 22.3 mm to 5.1 mm with an increment of 77.1%. It is concluded that increasing the tensile steel reinforcement ratio increased load carrying capacity and decreases ductility, as shown in Fig. 9.



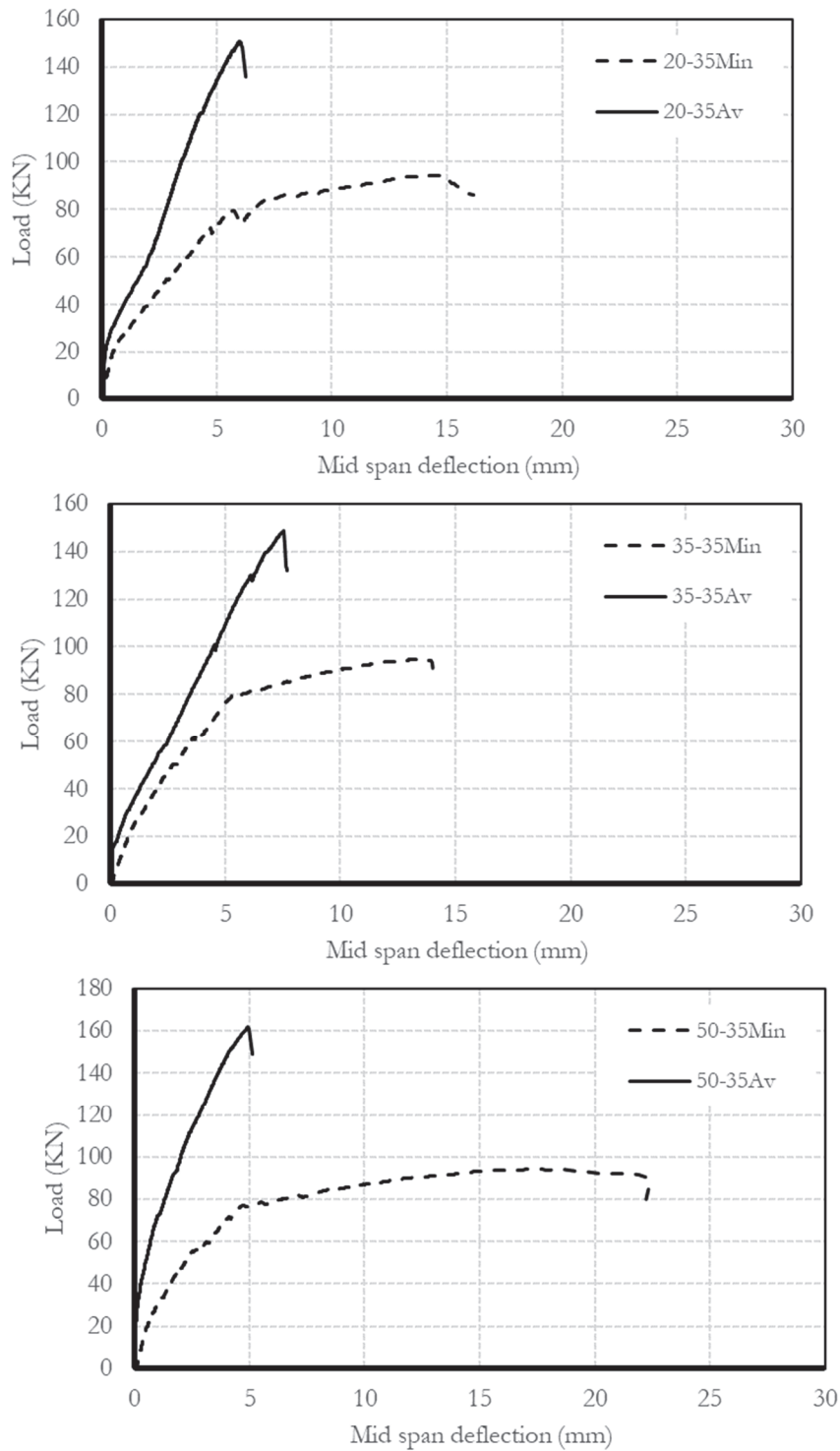


Figure 9: Load-deflection curve for beams with same layers of beam section and different  $A_s$ .

The failure modes of these beams are shown in Fig. 10. All beams with average steel reinforcement failed due to shear. Unlike the beams with average steel, the beams with a minimum steel showed a pronounced deflection after yielding up to failure.

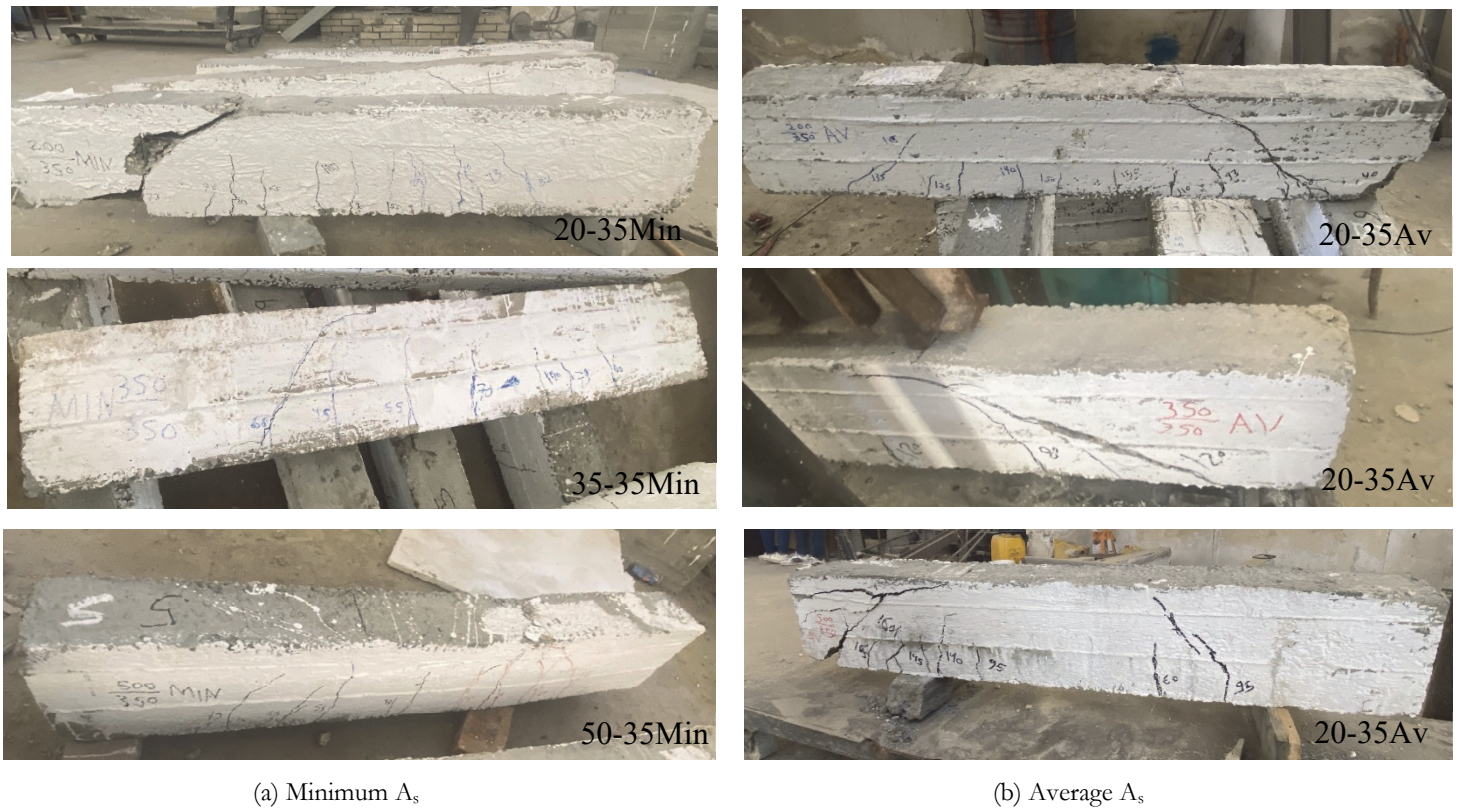


Figure 10: Crack pattern using concrete strength 35 MPa in tension zone and variation in Compression zone.

Fig. 11.a shows the load-deflection curve using beam 50-50Min as the control beam (Concrete strength 50 MPa with minimum  $A_s$ ). The strength of the compression zone in the other beams was 20 or 35 MPa. It was shown that the load capacity of beams decreases with low compressive strength in the compression zone with an increment of 23.4% and 5.4% using 20 and 50 MPa respectively. The deflection decreased by a percent 32.2% and 8.1% using 20 and 50 MPa respectively. It is concluded that using low strength in the compression zone decreases load carrying capacity and ductility. The beams with average steel reinforcement, the highest load carrying capacity recorded higher strength in the compression zone and decreased with percent 33.2% and 23.1% using 20 and 350MPa respectively. The deflection decreased with high strength in the compression zone. It is concluded that higher strength in the compression zone increases load carrying capacity and decreases deflection, as shown in Fig. 11.b.

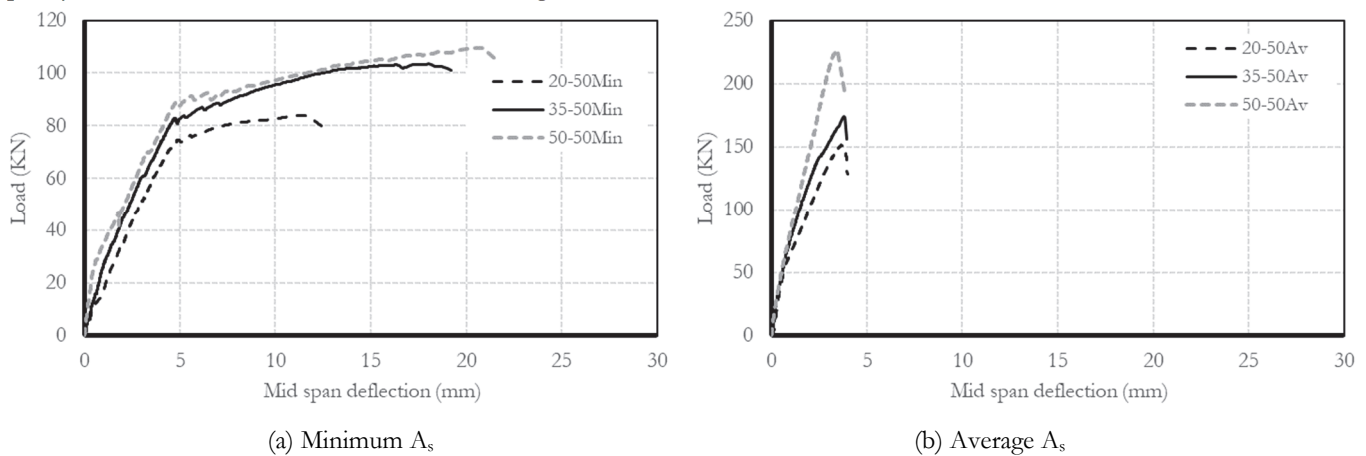


Figure 11: Load-deflection curve using concrete strength 50 MPa in tension zone and variation in Compression zone.

Like the beams of 20 and 35 MPa tension layer, the beams having the same layers and different reinforcement ratios showed the same trend of the average steel reinforcement ratios compared to the same minimum steel reinforcement ratios. The load capacity increased from 83.9 kN to 151.6 kN with an increment of 80.7%, and deflection decreased from 12.4 mm to

3.9 mm with an increment of 68% for beams 20-50 Min and Av. The percent of load capacity increase was 68.5%, and decreasing in deflection was 79.3% for beams 35-50 Min and Av. Similarly, for beams 50-50 Min and Av, the load capacity increased by 107.3%, and the deflection decreased by 82.1%. It is concluded that increasing the tensile steel reinforcement ratio increases load carrying capacity and decreases ductility, as shown in Fig. 12.

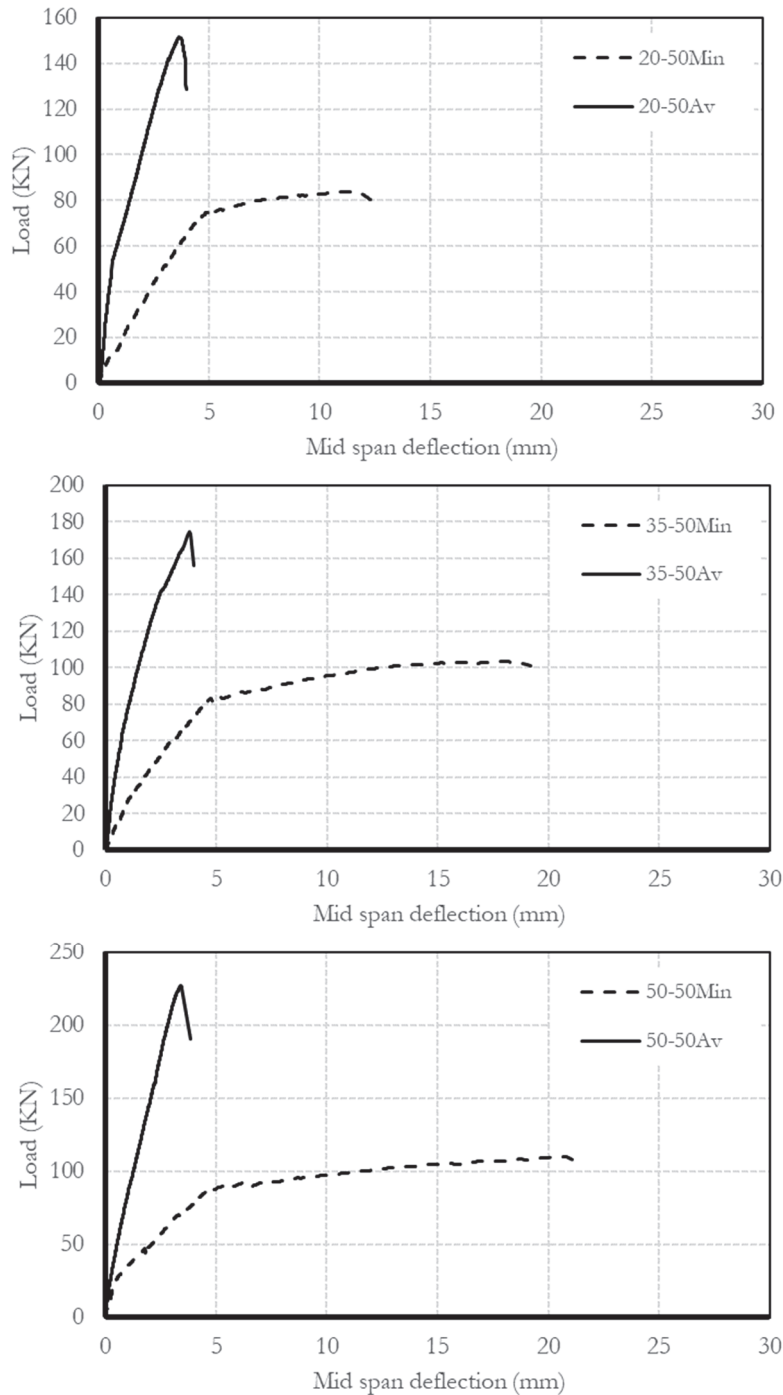


Figure 12: Load-deflection curve for beams with same layers of beam section and different  $A_s$ .

The failure modes of these beams are shown in Fig. 13. All beams with average steel reinforcement failed due to shear. The beams with minimum have pronounced deflection after yielding before failure. The failure mode of beams with minimum steel reinforcement was concrete crushing.



Figure 13: Crack pattern using concrete strength 50 MPa in tension zone and variation in Compression zone.

Fig. 14.a shows the maximum load with varying compression and tension zone strengths using minimum steel reinforcement. The horizontal axis is the strength in the compression zone, and the vertical is the maximum load. The highest load was recorded by using compressive strength 50 MPa in the compression zone with different strengths in the tension zone. The maximum deflection draws with varying strength, as shown in Fig. 14.b. Increasing compressive strength in the compression zone increases beams' deflection, increasing ductility.

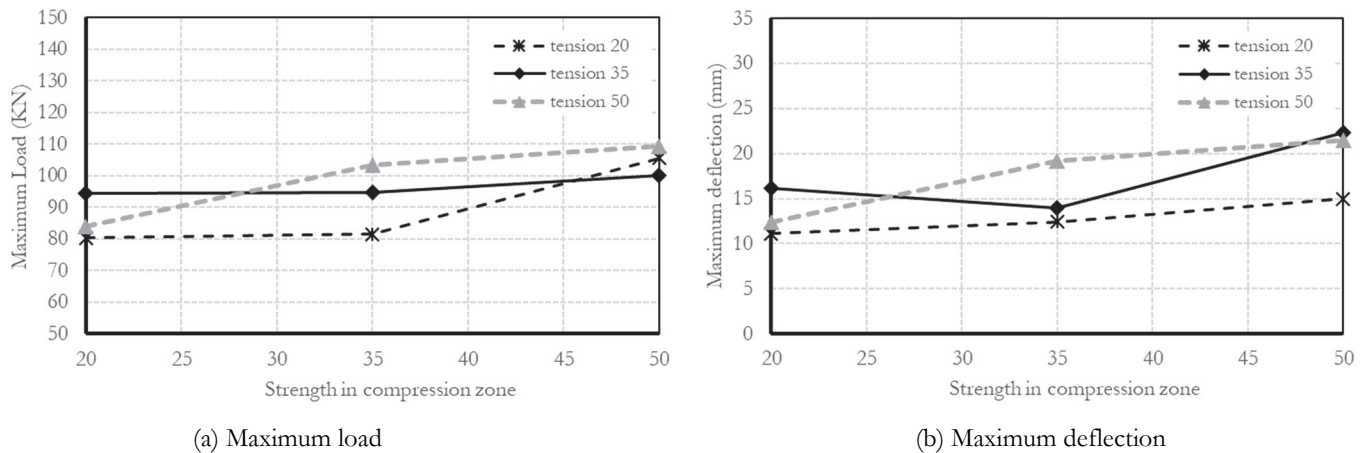


Figure 14: varying strength in compression and tension zones using minimum steel reinforcement.

Fig. 15.a shows the maximum load with varying strength in compression and tension zone using average steel reinforcement. The horizontal axis is the compression zone's strength, and the vertical axis is the maximum load. The highest load was recorded by using compressive strength 50 MPa in the compression zone with different strengths in the tension zone. The maximum deflection draws with varying strength as shown in Fig. 15.b. Increasing compressive strength in the compression zone decreases beams' deflection, leading to decrease ductility.

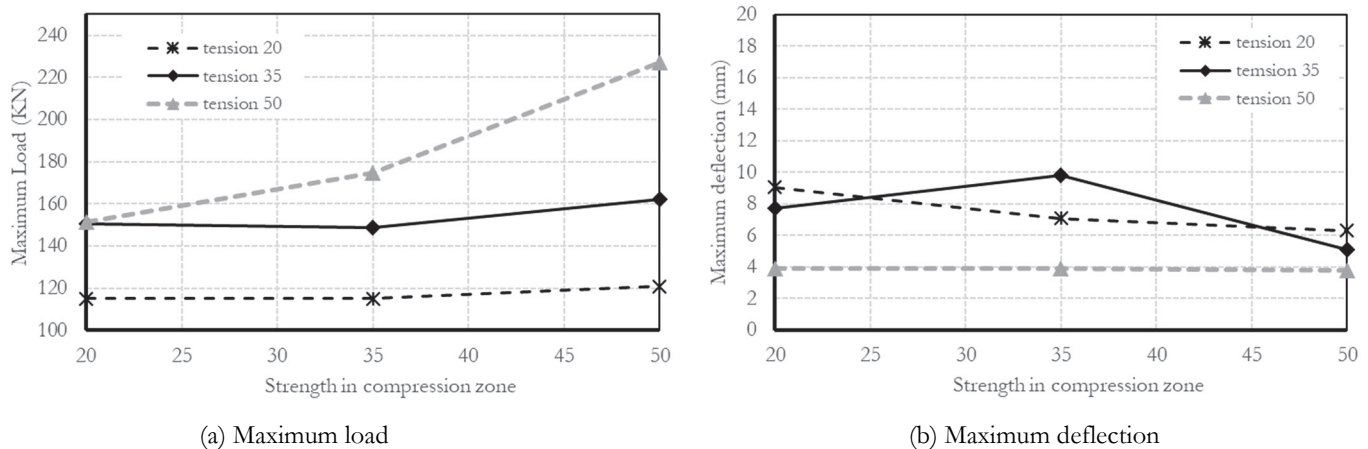


Figure 15: varying strength in compression and tension zones using Average steel reinforcement.

### NUMERICAL RESULTS AND COMPARISONS

A 3D finite element analysis was executed using ABAQUS to simulate the behavior of reinforced concrete beams tested in the experimental program [20]. The model consisted of two main parts; the concrete was modeled using 3D solid deformable element. The second main part was the steel which modeled using 1D axially loaded truss element [21], [22]. Concrete material defined elastic and concrete damage plasticity. The constitutive model, according to Carreira and Chu used for the definition of concrete as shown in Fig. 16.a, b [23], [24]. The concrete damage plasticity model was used to present the behavior of concrete in tension and compression. The plasticity parameters used are the dilation angle ( $\Psi$ ) with a value of 35 [25], eccentricity ( $\epsilon$ ) with a value of 0.1 [20], the ratio of initial equibiaxial compressive yield stress to initial uniaxial compressive yield stress ( $f_{b0}/f_{c0}$ ) with a value 1.16 [26], [27], the ratio of the second stress invariant on the tensile meridian ( $K_c$ ) with a value of 0.667 [26], Viscosity parameter ( $\mu$ ) with a value of 0.01 [25]. Steel was modeled as elastoplastic and linear hardening curve to describe yielding stage [21], [22]. A perfect bond between steel and concrete is assigned using the embedded region interaction. The element assigned to concrete was eight nodes element (C3D8R) and steel was two nodes element (T3D2).

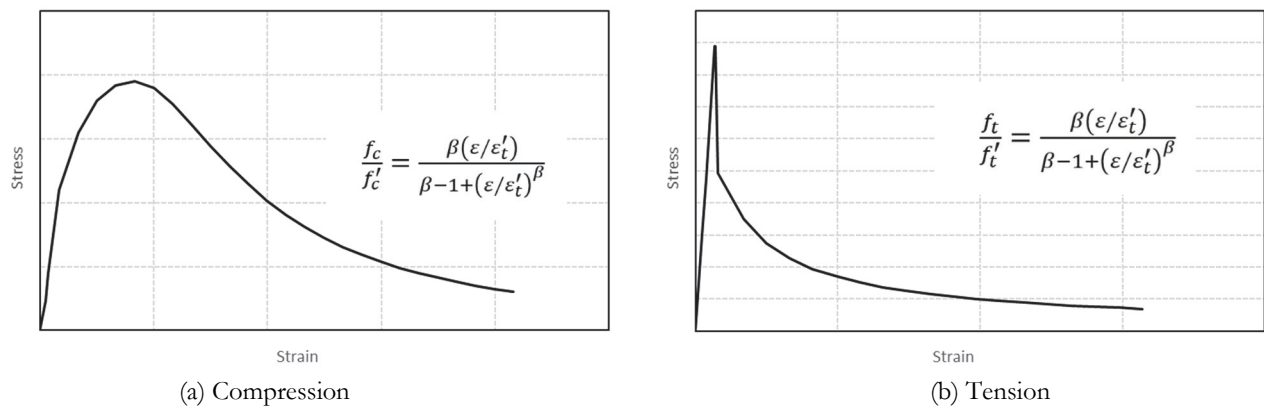
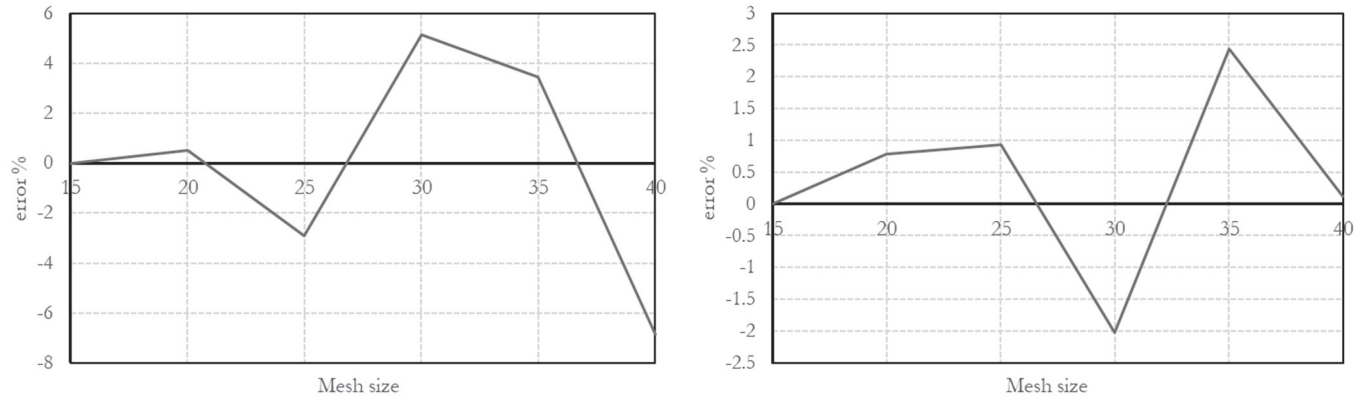


Figure 16: Constitutive model defines concrete damage plasticity.

Mesh sensitivity analysis was used to select the proper element size. The element sizes studied were 40,35,30,25,20,20 and 15mm. Load and deflection were studied at specific step time. According to the time cost and the accuracy of the results, the best element size was 20 mm with an error percent less than 1% compared to 15mm, see Fig. 17.



(a) Load at specific step time

(b) Deflection at specific step time

Figure 17: Mesh sensitivity analysis.

Verification was done on two beams from experimental work to confirm the result of the program. The two beams studied are 50-35 with minimum  $A_s$  and 50-50 with average  $A_s$ . The beam cross section is divided into two layers. The loading plate and supports are simulated as experimental, as shown in Fig. 18. The tensile steel, compression steel, and stirrups arrayed with spacing as experimental as shown in Fig. 19.

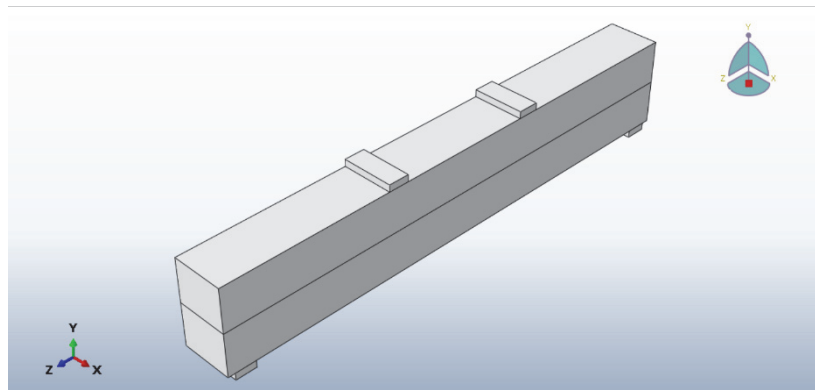


Figure 18: Simulation Beam, loading plates, and supports.

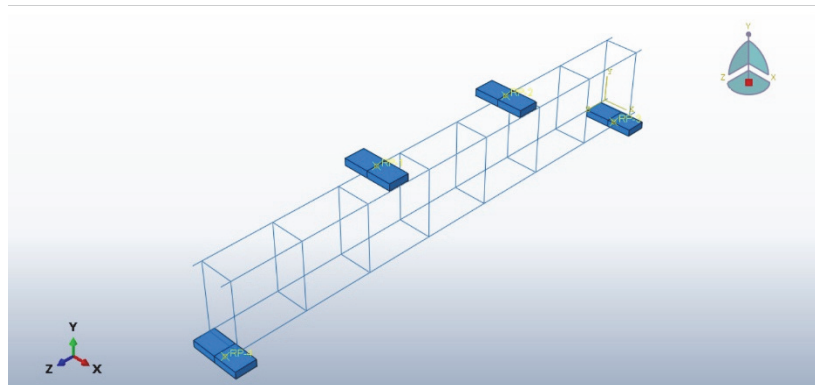


Figure 19: Simulation compression steel, tension steel, and stirrup.

The result showed that the beams have the same behavior in experimental and numerical. The difference between experimental and numerical curves was due to concrete shrinkage, casting environment, and non-homogeneity of concrete distribution as shown in Fig. 20.a, b.

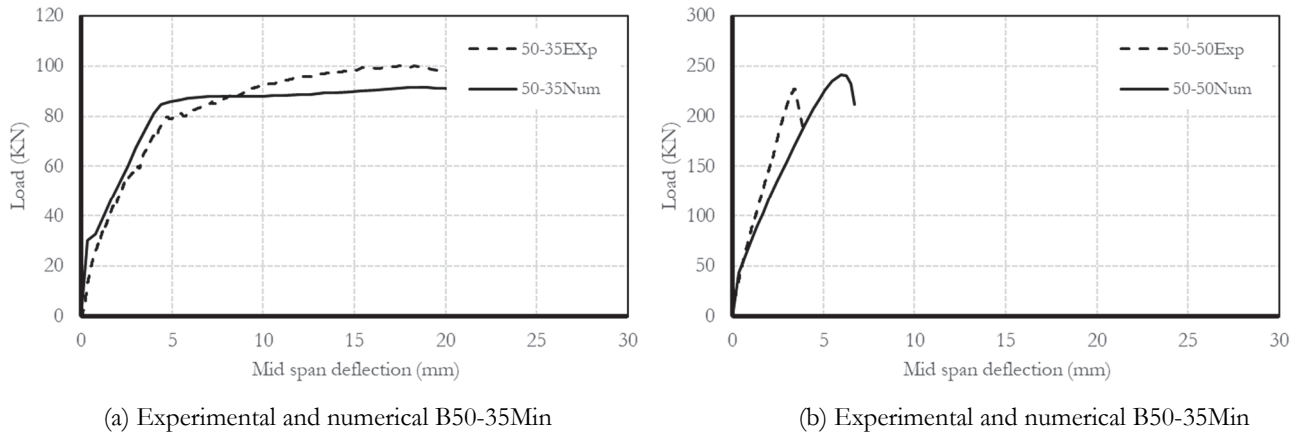


Figure 20: Verification model for two beams

The numerical load deflection curve using beam 20-20Min as a control beam with different strengths in the compression zone as shown in Fig. 21.a and Beam 20-20Av as a control beam with different strengths in the compression zone as shown in Fig. 21.b. The numerical result showed similar behavior of experimental beams. The numerical mode of failure was the same as the experimental, as shown in Fig. 22.

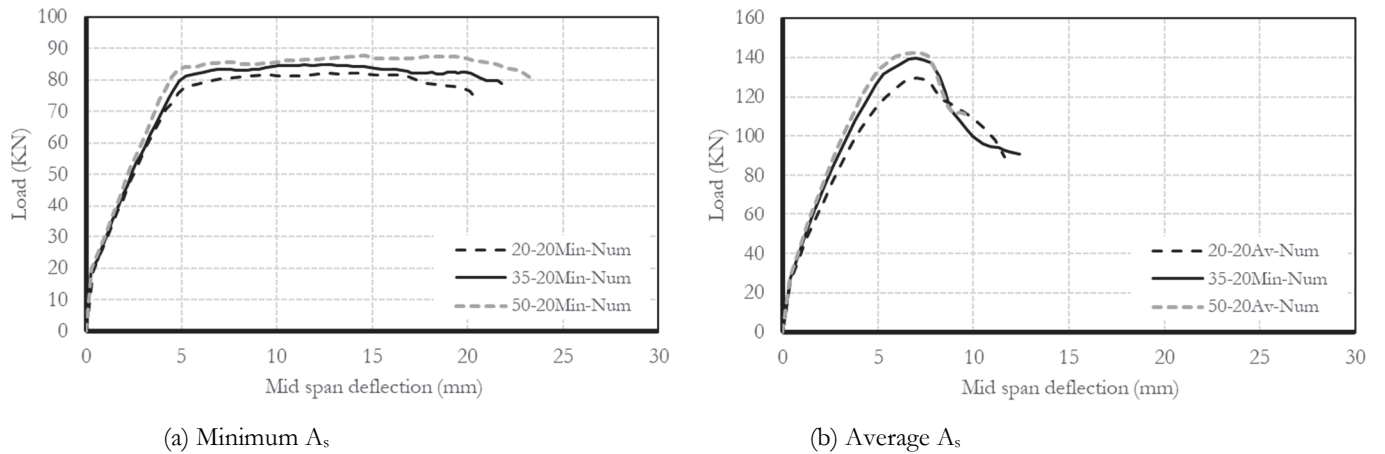


Figure 21: Numerical load-deflection curve using concrete strength 20 MPa in tension zone and variation in Compression zone.

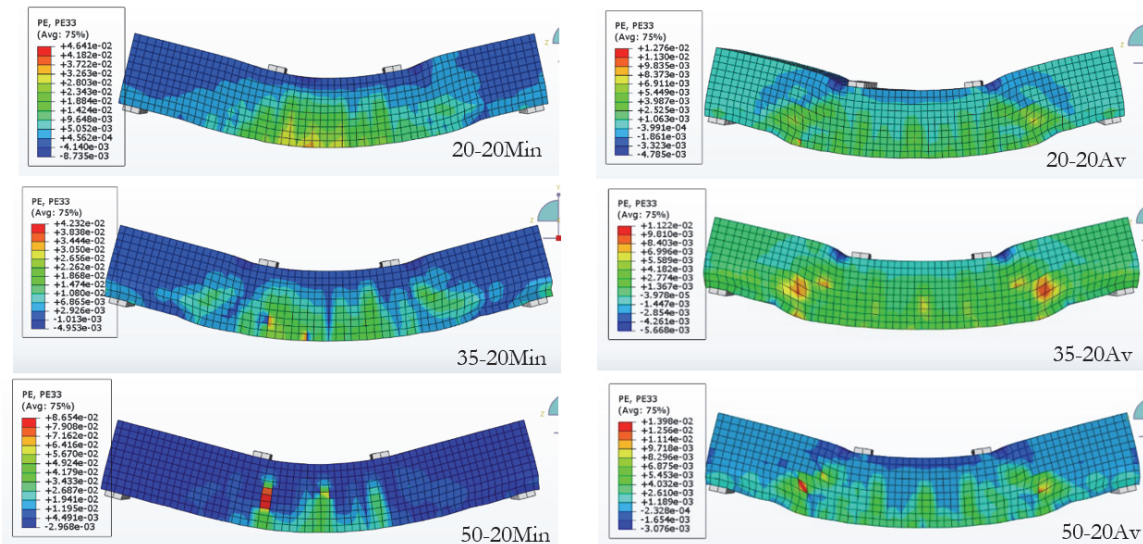


Figure 22: Numerical modes of failure presented by Plastic strain contour for concrete strength 20 MPa in tension zone and variation in Compression.

The numerical load deflection curve using beam 35-35Min as the control beam with different strength in the compression zone as shown in Fig. 23.a. Beam 35-35Av as the control beam with different strength in the compression zone as shown in Fig. 23.b. The numerical result showed similar behavior of experimental beams. The numerical mode of failure was the same as the experimental, as shown in Fig. 24.

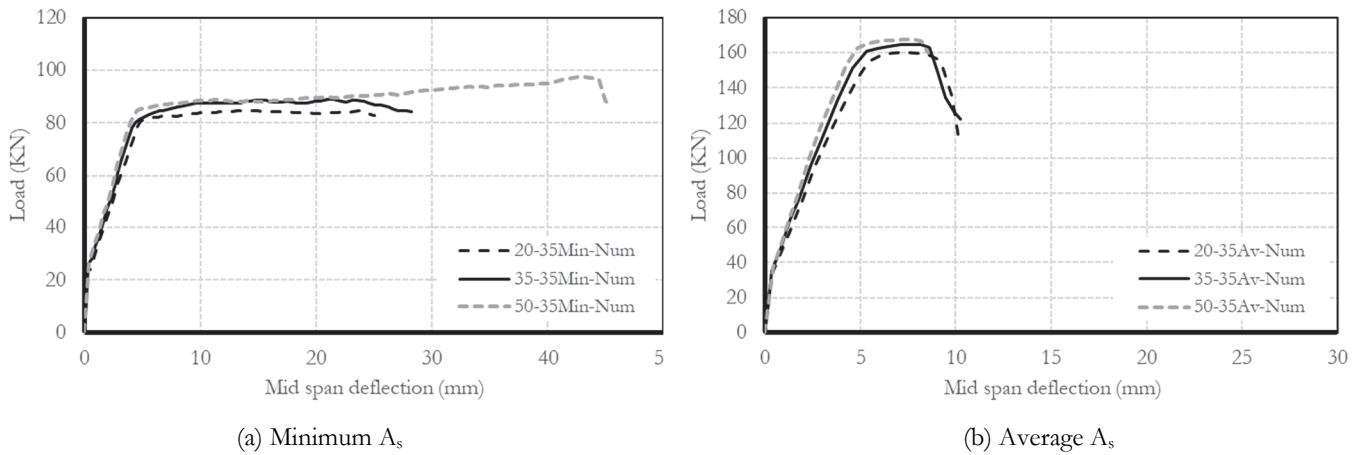


Figure 23: Numerical load-deflection curve using concrete strength 35 MPa in tension zone and variation in Compression zone.

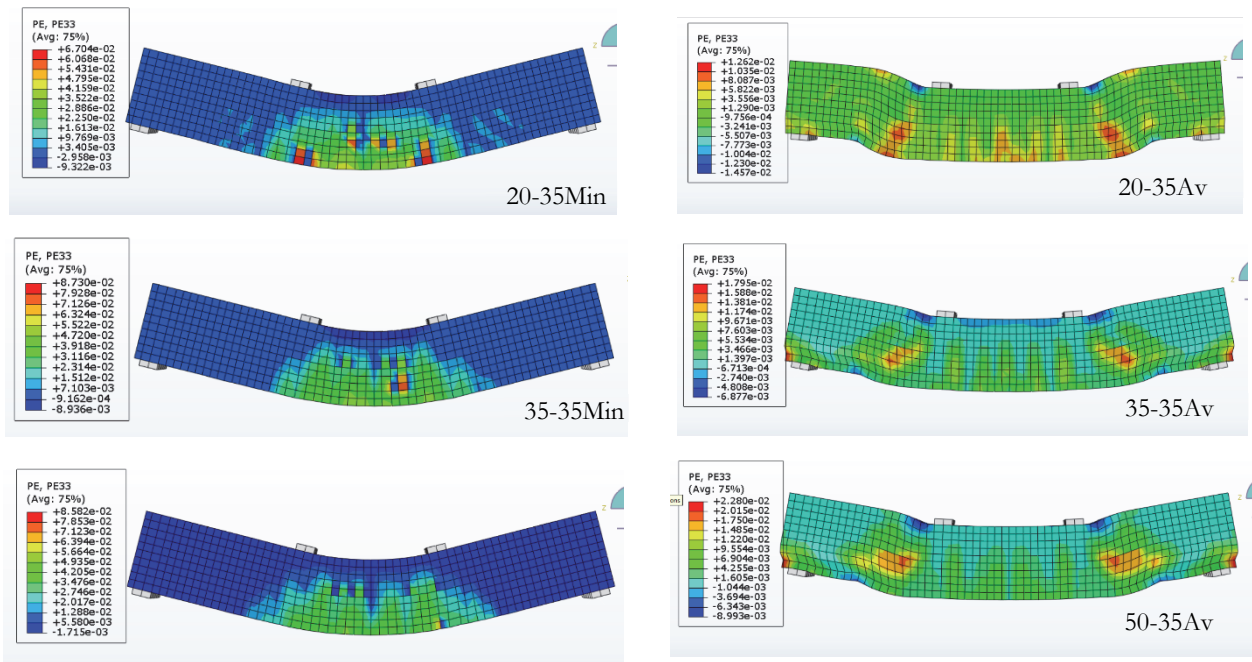


Figure 24: Numerical modes of failure presented by Plastic strain contour for concrete strength 35 MPa in tension zone and variation in Compression.

The numerical load deflection curve using beam 35-35Min as the control beam with different strength in the compression zone as shown in Fig. 25.a. Beam 35-35Av as control beam with different strengths in the compression zone as shown in Fig. 25.b. The numerical result showed similar behavior of experimental beams. The numerical mode of failure was the same as the experimental, as shown in Fig. 26.



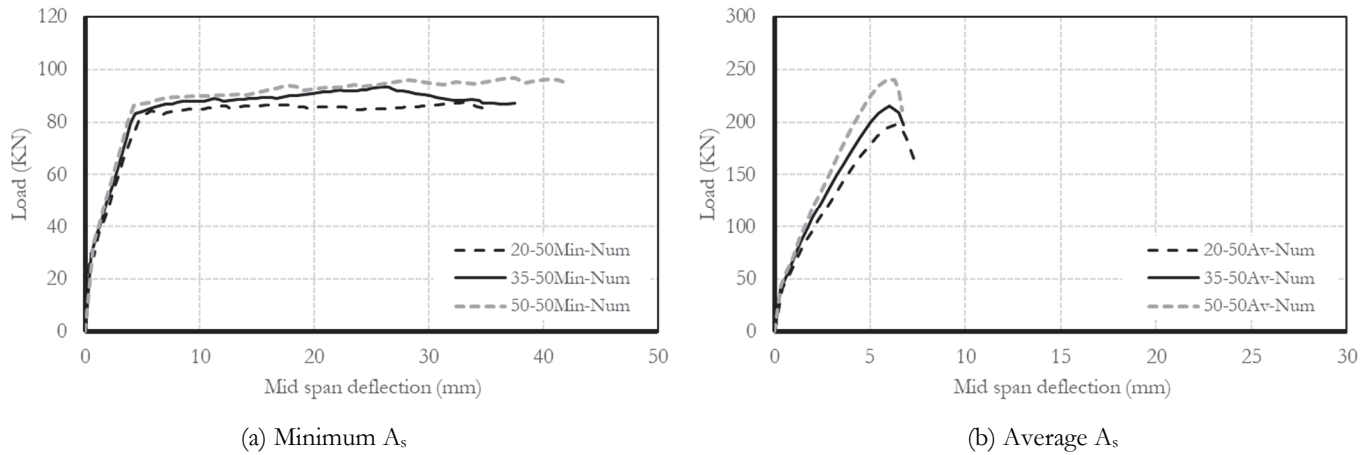


Figure 25: Numerical load-deflection curve using concrete strength 50 MPa in tension zone and variation in Compression zone.

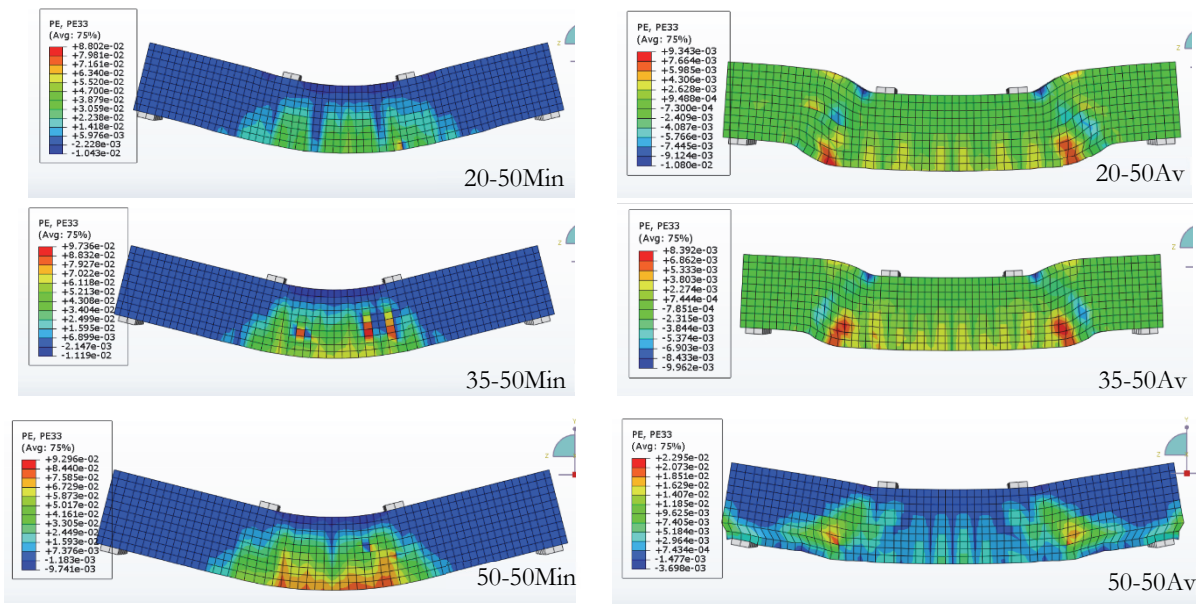


Figure 26: Numerical modes of failure presented by Plastic strain contour for concrete strength 50 MPa in tension zone and variation in Compression.

## CONCLUSIONS

- An experimental and numerical study was done on eighteen reinforced concrete beams with different compressive strengths and different ratios of steel reinforcement and the result showed that:
- Increasing tensile steel reinforcement from minimum to average leads to increase load carrying capacity and decreased ductility for the same cross-section configuration.
  - The load carrying capacity was found to increase with higher strength of concrete in the compression zone for minimum or average steel reinforcement.
  - The deflection was found to increase with higher strength in the compression zone at minimum steel reinforcement from 35 to 37.1% at strength 50 MPa in the compression zone.
  - The deflection was found to decrease with higher strength in the compression zone at average steel reinforcement from 6.3 and 2.6% at strength 50 MPa in the compression zone.
  - The failure mode of all beams with average steel reinforcement was due to shear.
  - Increasing the value of strength in the compression zone can be used for beams with high steel reinforcement ratios which decreases compression steel.



- The experimental and numerical results were found not identical in values; however, they had similar behavior.

## REFERENCES

- [1] Pratama, M. M. A., Arifanda, W., Karyadi, K., Nindyawati, N., Sulaksitaningrum, R. and Prayuda, H. (2019). Numerical and experimental investigation on the shear resistance of functionally graded concrete (FGC) beams, in IOP Conference Series: Materials Science and Engineering, Institute of Physics Publishing, DOI: 10.1088/1757-899X/669/1/012055.
- [2] Naghibdehi, M. G., Mastali, M., Sharbatdar, M. K., and Naghibdehi, M. G. (2014). Flexural performance of functionally graded RC cross-section with steel and PP fibres, *Magazine of Concrete Research*, 66(5), pp. 219–233. DOI: 10.1680/macr.13.00248.
- [3] Othman, M. A., El-Emam El-Emam, H. M., Seleem, M. H., Sallam, H. E. M., and Moawad, M., (2021). Flexural behavior of functionally graded concrete beams with different patterns, *Archives of Civil and Mechanical Engineering*, 21(4), DOI: 10.1007/s43452-021-00317-0.
- [4] Shirai, K., Horii, J., Nakamuta, K. and Teo, W. (2022). Experimental investigation on the mechanical and interfacial properties of fiber-reinforced geopolymer layer on the tension zone of normal concrete, *Constr. Build Mater*, 360, DOI: 10.1016/j.conbuildmat.2022.129568.
- [5] Ho, J. C. M., Kwan, A. K. H., and Pam, H. J. (2002). Effects of using high-strength concrete on flexural ductility of reinforced concrete beams, *HKIE Transactions*, 9(1), pp. 14–21.
- [6] Olivia, M. and Mandal, P. (2005). Curvature ductility of reinforced concrete beam, *Journal of Civil Engineering*, 6(1), pp. 1–13.
- [7] Mansor, A. A., Mohammed, A. S., and Salman, W. D. (2020). Effect of longitudinal steel reinforcement ratio on deflection and ductility in reinforced concrete beams, in IOP Conference Series: Materials Science and Engineering, IOP Publishing, p. 012008.
- [8] Graf, A. A., Bneni, M. A., El-Kholy, E.-M. I., Elkilani, A. and Ahmad, S. S. E. (2022). Experimental and numerical evaluation of compression confinement techniques for HSC beams reinforced with different ratios of high strength steel reinforcement, *Frattura e Integrità Strutturale*, 60, pp. 310-330. DOI: 10.3221/IGF-ESIS.60.22.
- [9] Li, K., Wei, Y., Li, Y., Li, Z. and Zhu, J., (2023). Flexural behavior of reinforced concrete beams strengthened with high-strength stainless steel wire rope meshes reinforced ECC, *Constr Build Mater*, 362, DOI: 10.1016/j.conbuildmat.2022.129627.
- [10] Kwan, A. K. H., Chau, S. L. and Au, F. T. K. (2006). Improving flexural ductility of high-strength concrete beams, *Proceedings of the Institution of Civil Engineers-Structures and Buildings*, 159(6), pp. 339–347.
- [11] Ashour, S. A., Waf, a F. F. and Kamal, M. I., (2000). Effect of the concrete compressive strength and tensile reinforcement ratio on the flexural behavior of fibrous concrete beams, 22(9), pp. 1145-1158. DOI: 10.1016/S0141-0296(99)00052-8
- [12] Gümüş, M. and Arslan, A. (2018). Effect of fiber type and content on the flexural behavior of high strength concrete beams with low reinforcement ratios, *Structures*, 20, pp. 1–10, DOI: 10.1016/j.istruc.2019.02.018.
- [13] Yoo, D.-Y., Banthia, N. and Yoon, Y.-S. (2017). Experimental and numerical study on flexural behavior of ultra-high-performance fiber-reinforced concrete beams with low reinforcement ratios, *Canadian Journal of Civil Engineering*, 44(1), pp. 18–28.
- [14] Ministry of Housing, U. & U. C., ECP 203, (2020), *The Egyptian Code for Design and Construction of Concrete Structures*.
- [15] ISO, ISO 6935-2: (2019). *Steel for the reinforcement of concrete — Part 2: Ribbed bars*.
- [16] ACI PRC-211.1-91: (2009). *Standard Practice for Selecting Proportions for Normal, Heavyweight, and Mass Concrete*.
- [17] British Standards Institution, *Testing hardened concrete. Part 3, (2009) Compressive strength of test specimens*.
- [18] British Standard, *Testing hardened concrete Part 6: (2010). Tensile splitting strength of test specimens*.
- [19] British Standard, *Testing hardened concrete Part 5: (2009). Flexural strength of test specimens*.
- [20] Dassault S., (2014). *ABAQUS 6.14 analysis User's Manual*, Dassault Systems: Providence, RI, USA.
- [21] Maio, U. De, Gaetano, D., Greco, F., Lonetti, P. and Pranno, A. (2023). The damage effect on the dynamic characteristics of FRP-strengthened reinforced concrete structures, *Compos Struct*, 309, p. 116731, DOI: 10.1016/j.compstruct.2023.116731.
- [22] Maio, U. De, Gaetano, D. Greco, F., Lonetti, P., Nevone Blasi, P., and Pranno, A., (2023). The Reinforcing Effect of Nano-Modified Epoxy Resin on the Failure Behavior of FRP-Plated RC Structures, *Buildings*, 13(5), p. 1139.



- [23] Carreira, D. J. and Chu, K.-H., (1985). Stress-strain relationship for plain concrete in compression, *Journal Proceedings*, pp. 797–804.
- [24] Carreira, D. J. and Chu, K.-H. (1986). Stress-strain relationship for reinforced concrete in tension, *Journal Proceedings*, pp. 21–28.
- [25] Tao, Z., Wang, Z.-B. and Yu, Q. (2013). Finite element modelling of concrete-filled steel stub columns under axial compression, *J Constr Steel Res*, 89, pp. 121–131.
- [26] Lee, S.-H., Abolmaali, A., Shin, K.-J. and Lee, H.-D. (2020). ABAQUS modeling for post-tensioned reinforced concrete beams, *Journal of Building Engineering*, 30, p. 101273.
- [27] Seow, P. E. C. and Swaddiwudhipong, S. (2005). Failure surface for concrete under multiaxial load—A unified approach, *Journal of materials in civil engineering*, 17(2), pp. 219–228.